Supplemental Information

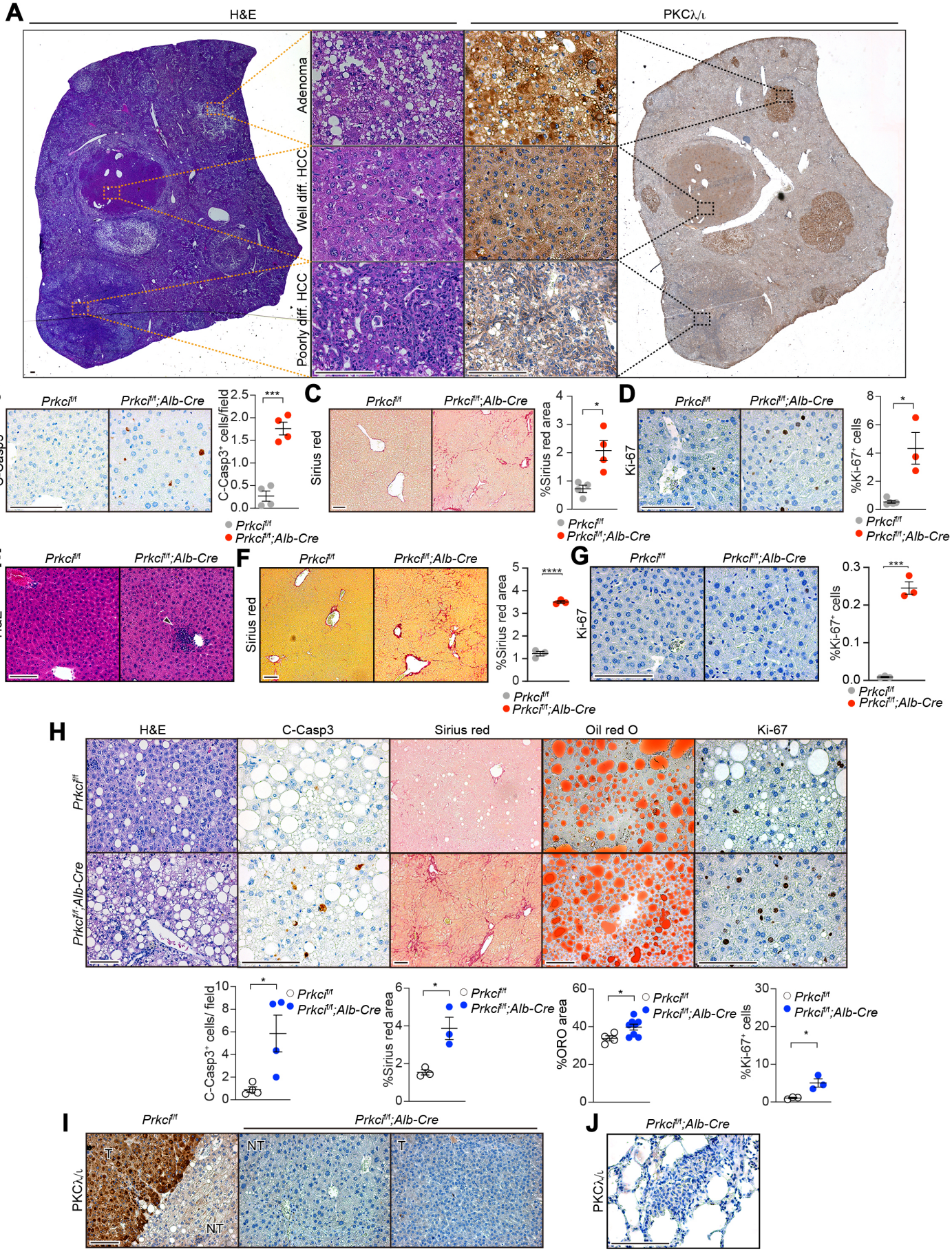

Figure S1. PKCλ/ι Ablation in Hepatocytes Increase Liver Injury and Fibrosis, Related to Figure 1

(A) Representative H&E staining and IHC for PKCλ/ι of hepatic tumor sections from wild-type mice at 36 weeks of age treated under DEN/HFD protocol. (B) IHC for cleaved caspase-3 (C-Casp3) in livers from *Prkci*$^{f/f}$ and *Prkci*$^{f/f}$;*Alb-Cre* mice at 30 weeks of age, and quantification of the number C-Casp3^{+} hepatocytes per field (n = 4). (C) Sirius red staining in *Prkci*$^{f/f}$ and *Prkci*$^{f/f}$;*Alb-Cre* livers and quantification of the Sirius red-positive area per field (n = 4). (D) IHC for Ki-67 in *Prkci*$^{f/f}$ (n = 5) and *Prkci*$^{f/f}$;*Alb-Cre* (n = 3) livers and quantification of the number of Ki-67 positive (Ki-67^{+}) hepatocytes. (E) H&E staining of livers from older *Prkci*$^{f/f}$ and *Prkci*$^{f/f}$;*Alb-Cre* mice (age range 33-52 weeks). Arrow heads indicate a cellular infiltrate. Scale bar, 100 μm. (F) Sirius red staining in *Prkci*$^{f/f}$ and *Prkci*$^{f/f}$;*Alb-Cre* livers from older animals and quantification of the Sirius red-positive area per field (n = 3). (G) IHC for Ki-67 in *Prkci*$^{f/f}$ and *Prkci*$^{f/f}$;*Alb-Cre* livers from older animals and quantification of the number of Ki-67 positive (Ki-67^{+}) hepatocytes (n = 3). (H) H&E staining, IHC for C-Casp3, Sirius red staining, Oil red O staining, and IHC for Ki-67 in *Prkci*$^{f/f}$ and *Prkci*$^{f/f}$;*Alb-Cre* livers subjected to DEN/HFD protocol (n = 3-8 per group), and quantification of the number of positive cells or the positive area per field. (I and J) IHC for PKCλ/ι in *Prkci*$^{f/f}$ and *Prkci*$^{f/f}$;*Alb-Cre* livers subjected to DEN/HFD protocol, including tumors (T) and background non-tumorous tissues (NT) (I) and lung metastasis in *Prkci*$^{f/f}$;*Alb-Cre* mice (J). Results are presented as mean ± SEM. *$p < 0.05$, **$p < 0.01$, ***$p < 0.001$. Scale bars, 100 μm.

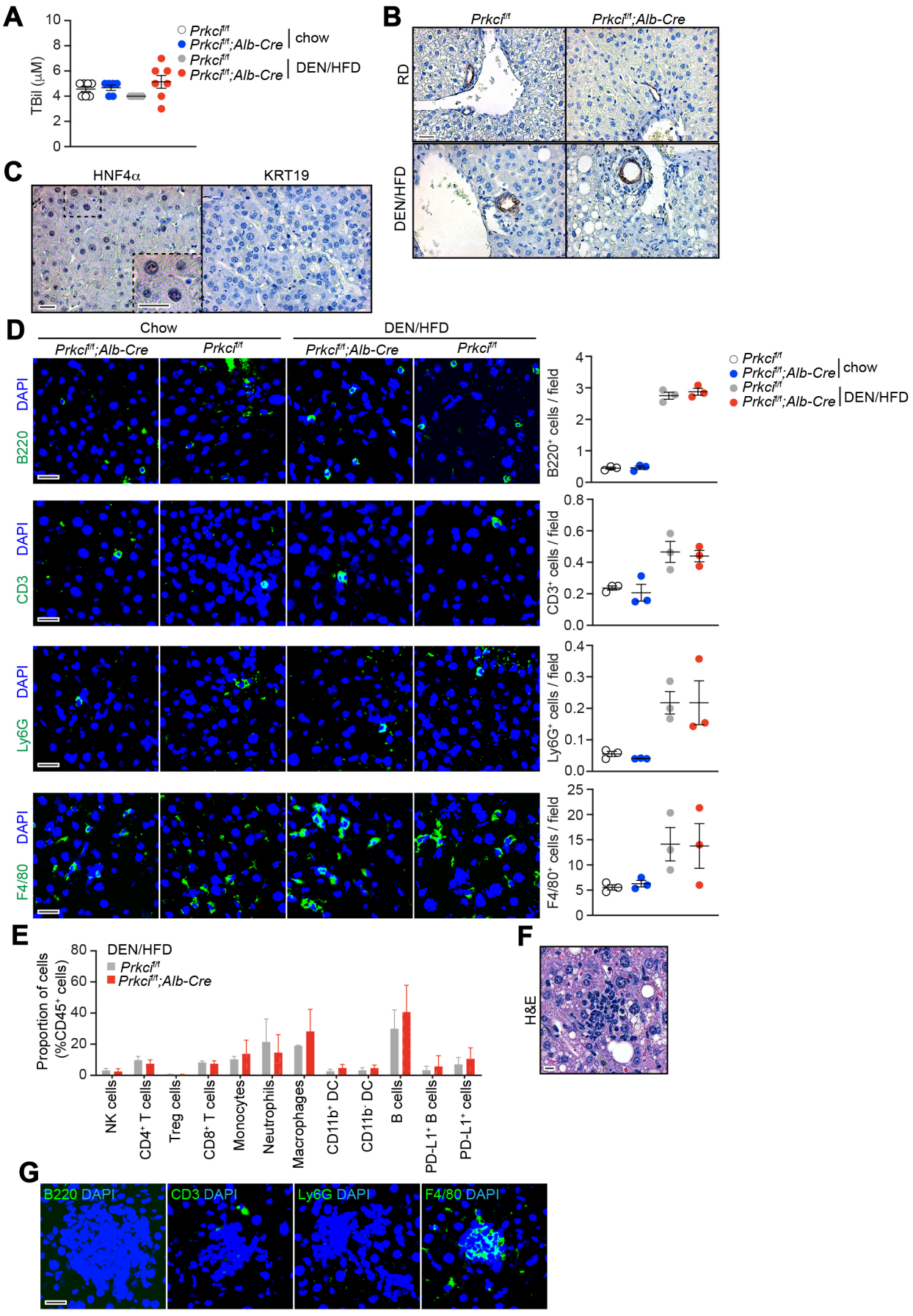
A
TBil (μM)
Prkci f/f
Prkci f/f;Alb-Cre | chow
Prkci f/f
Prkci f/f;Alb-Cre | DEN/HFD
B
Prkci f/f
Prkci f/f;Alb-Cre
RD
DEN/HFD
C
HNF4α
KRT19
D
Chow
DEN/HFD
Prkci f/f;Alb-Cre
Prkci f/f
DAPI
B220
CD3
Ly6G
F4/80
B220+ cells / field
CD3+ cells / field
Ly6G+ cells / field
F4/80+ cells / field
E
DEN/HFD
Prkci f/f
Prkci f/f;Alb-Cre
Proportion of cells (%CD45+ cells)
NK cells
CD4+ T cells
Treg cells
CD8+ T cells
Monocytes
Neutrophils
Macrophages
CD11b+ DC
CD11b- DC
B cells
PD-L1+ B cells
PD-L1+ cells
F
H&E
G
B220 DAPI
CD3 DAPI
Ly6G DAPI
F4/80 DAPI

Figure S2. Loss of PKCλ/ι in Hepatocytes Does Not Alter the Cholangiocellular Compartment or Inflammatory populations, Related to Figure 1

(A and B) Serum total bilirubin (TBil) levels (A) and IHC for keratin 19 (KRT19) (B) in livers from *Prkci*$^{f/f}$ and *Prkci*$^{f/f}$;*Alb-Cre* male mice fed chow diet (RD) or under DEN/HFD protocol (n = 5-8). (C) IHC for hepatocyte nuclear factor 4α (HNF4α) and KRT19 in tumors developed in *Prkci*$^{f/f}$;*Alb-Cre* male mice subjected to DEN/HFD protocol. (D) Inflammatory infiltrates in *Prkci*$^{f/f}$ and *Prkci*$^{f/f}$;*Alb-Cre* livers from chow diet condition (30 weeks old) and DEN/HFD protocol (36 weeks old). The number of B cells (B220), T cells (CD3), monocytes and (neutrophilic) granulocytes (Ly6G), and macrophages and Kupffer cells (F4/80) were quantified by IF. (E) Quantification of immune cells in liver tissues from *Prkci*$^{f/f}$ and *Prkci*$^{f/f}$;*Alb-Cre* mice in DEN/HFD protocol via flow cytometry. (F) Representative image of small inflammatory infiltrates observed in mouse liver tissues. (G) IF for detection of B cells (B220), T cells (CD3), monocytes and (neutrophilic) granulocytes (Ly6G), and macrophages and Kupffer cells (F4/80) in small cellular infiltrates in mouse liver tissues. Results are presented as mean ± SEM. Scale bars, 25 μm (B and C); 10 μm (D, F, and G).

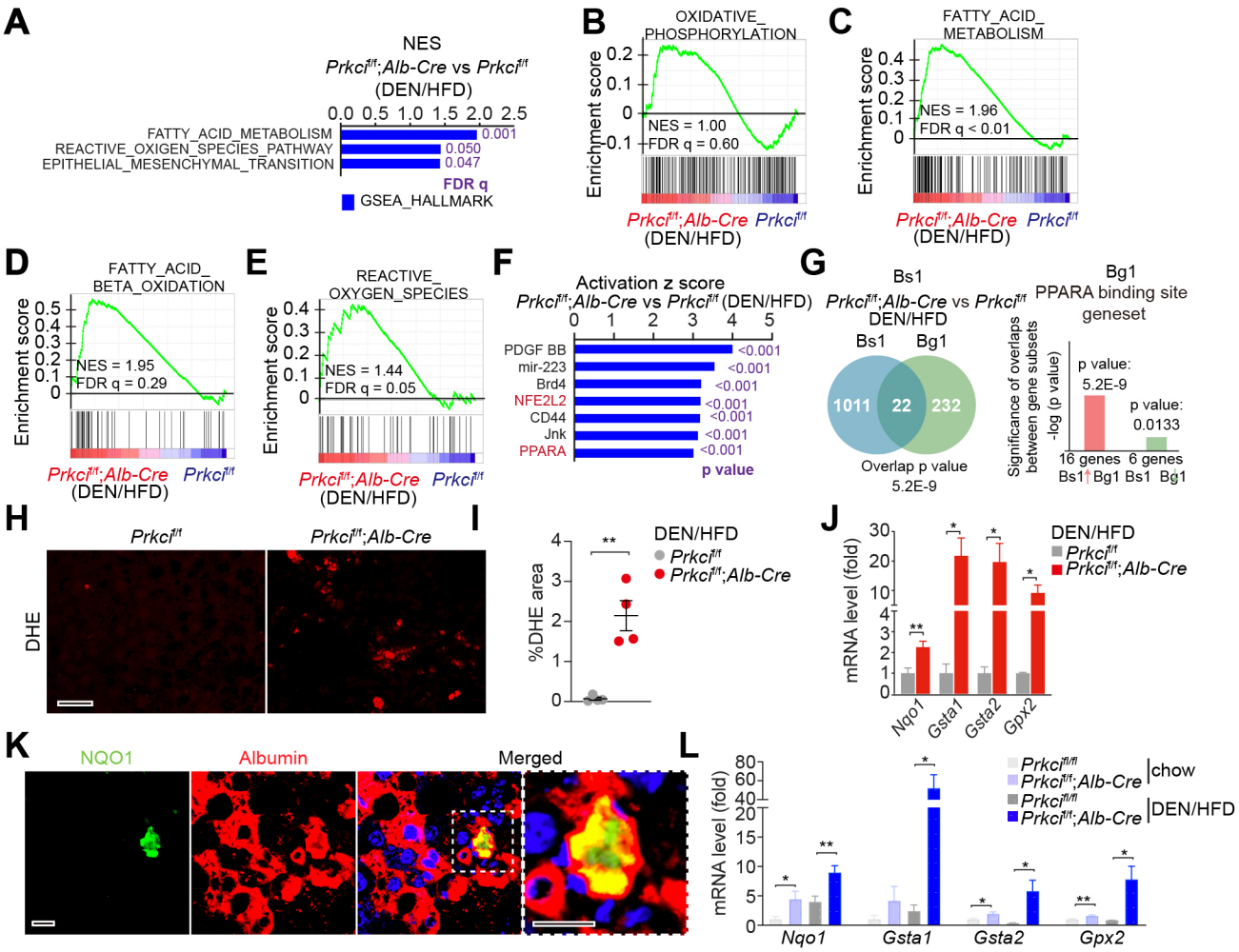

Figure S3. Loss of PKCλ/ι Increases PPARα and NRF2 Pathway Genes Expression, Related to Figure 2

(A-E) Upregulated pathways in *Prkci*$^{f/f}$;*Alb-Cre* livers (n =3) vs *Prkci*$^{f/f}$ livers (n = 4) subjected to DEN/HFD protocol using GSEA with Hallmark (GSEA_H) MSigDB database (A) and GSEA plots of enrichment in "HALLMARK_OXIDATIVE_PHOSPHORYLATION" (B), "HALLMARK_FATTY_ACID_METABOLISM" (C), "GO_FATTY_ACID_BETA_OXIDATION" (D), and "HALLMARK_REACTIVE_OXYGEN_SPIECIES" (E). (F) Upstream Regulator Analysis by IPA in *Prkci*$^{f/f}$;*Alb-Cre* livers (n =3) vs *Prkci*$^{f/f}$ livers (n = 4) subjected to DEN/HFD protocol. (G) NextBio analysis of gene overlap between genes upregulated in *Prkci*$^{f/f}$;*Alb-Cre* livers (n = 3) vs *Prkci*$^{f/f}$ livers (n = 4) subjected to DEN/HFD protocol (Bioset1, Bs1) and PPARα binding gene set (Biogroup 1, Bg1). (H and I) DHE assay in *Prkci*$^{f/f}$ and *Prkci*$^{f/f}$;*Alb-Cre* livers (n = 4) subjected to DEN/HFD protocol analyzed by IF microscopy (H) and quantification of the positive area per field (I). (J) qRT-PCR analysis of ROS-related genes in *Prkci*$^{f/f}$ (n = 6) and *Prkci*$^{f/f}$;*Alb-Cre* (n = 8) livers subjected to DEN/HFD protocol. (K) IF for NQO1 and albumin in *Prkci*$^{f/f}$;*Alb-Cre* liver from DEN/HFD protocol. Nuclei were stained by DAPI (blue). (L) qRT-PCR analysis of ROS-related genes in *Prkci*$^{f/f}$ (n = 6) and *Prkci*$^{f/f}$;*Alb-*

Cre (n = 8) livers subjected to RD or DEN/HFD protocol. The expression levels were normalized to *Prkci*$^{f/f}$ -RD. Results are presented as mean ± SEM. *p < 0.05, **p < 0.01. Scale bars, 25 μm.

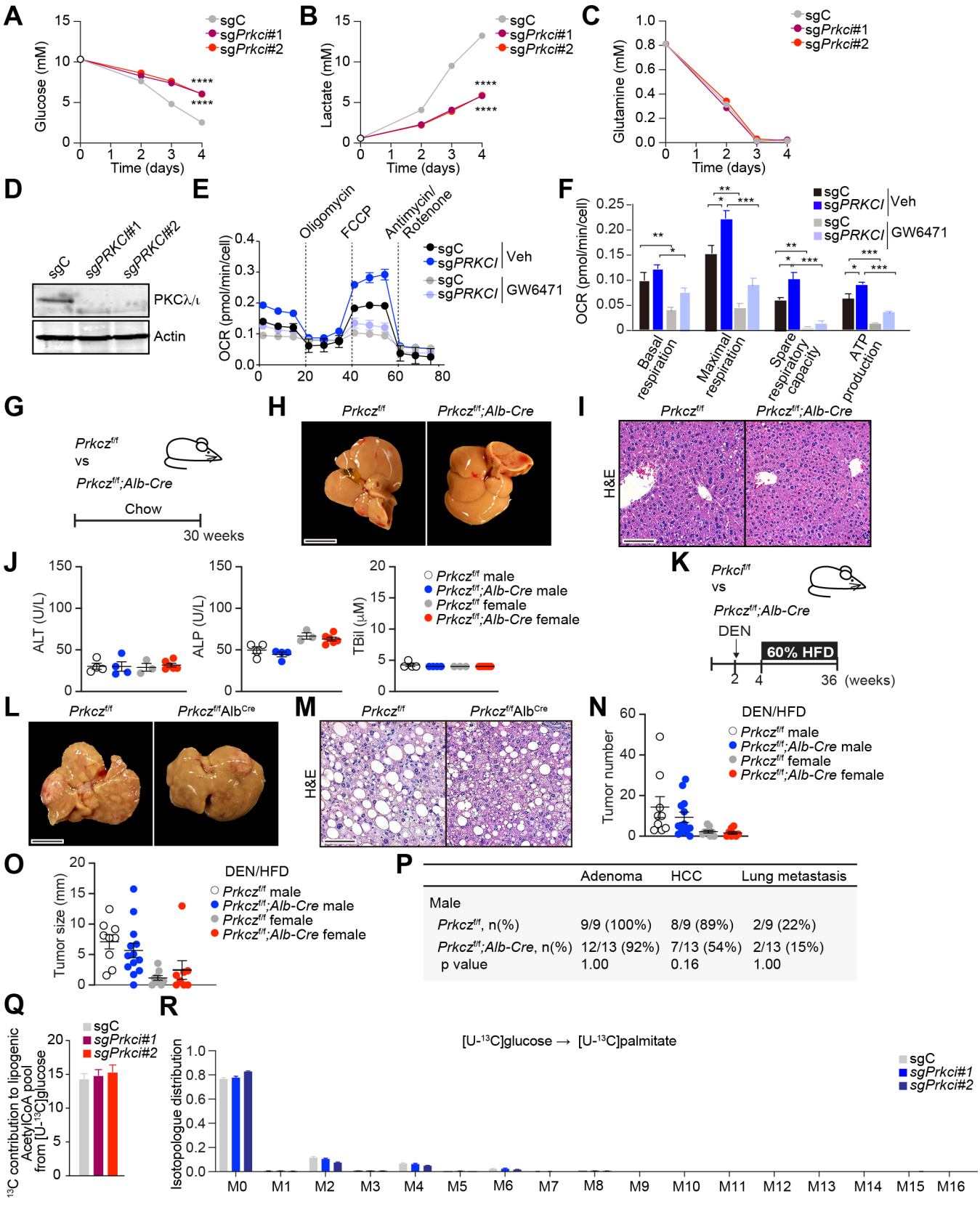
A
Glucose (mM)
Time (days)
sgC
sgPrkci#1
sgPrkci#2
****
B
Lactate (mM)
C
Glutamine (mM)
D
sgC
sgPRKCI#1
sgPRKCI#2
PKCλ/ι
Actin
E
OCR (pmol/min/cell)
Oligomycin
FCCP
Antimycin/ Rotenone
sgPRKCI
Veh
GW6471
F
Basal respiration
Maximal respiration
Spare respiratory capacity
ATP production
G
Prkcz f/f
vs
Prkcz f/f;Alb-Cre
Chow
30 weeks
H
Prkcz f/f
Prkcz f/f;Alb-Cre
I
H&E
J
ALT (U/L)
ALP (U/L)
TBil (μM)
Prkcz f/f male
Prkcz f/f;Alb-Cre male
Prkcz f/f female
Prkcz f/f;Alb-Cre female
K
Prkci f/f
vs
Prkcz f/f;Alb-Cre
DEN
60% HFD
2
4
36 (weeks)
L
Prkcz f/f
Prkcz f/f Alb Cre
M
H&E
N
Tumor number
DEN/HFD
O
Tumor size (mm)
DEN/HFD
P
Adenoma
HCC
Lung metastasis
Male
Prkcz f/f, n(%) 9/9 (100%) 8/9 (89%) 2/9 (22%)
Prkcz f/f;Alb-Cre, n(%) 12/13 (92%) 7/13 (54%) 2/13 (15%)
p value 1.00 0.16 1.00
Q
13C contribution to lipogenic Acetyl-CoA pool from [U-13C]glucose
R
[U-13C]glucose → [U-13C]palmitate
Isotopologue distribution
M0 M1 M2 M3 M4 M5 M6 M7 M8 M9 M10 M11 M12 M13 M14 M15 M16

Figure S4. PPARα Activity is Required for Enhanced OXPHOS in PKCλ/ι Deficient Hepatocytes, Related to Figure 3

(A-C) Glucose (A), lactate (B) and glutamine (C) levels in the media of sg*Prkci* (#1 and #2) and sgC BNL CL.2 cells cultured in complete media (n = 3). (D) Immunoblotting for PKCλ/ι and actin in CRISPR/Cas9-mediated *PRKCI* gene KO (sg*PRKCI*#1 and #2) or control (sgC) HepG2 cells. (E and F) OCR measurement on Seahorse (E) and calculation of different types of respiration (F) in sg*PRKCI* and sgC HepG2 cells (n = 3) treated with GW6471 (10 μM) or DMSO control (Veh) for 24 hours prior to and through the measurement. (G-J) Analyses of *Prkcz*$^{f/f}$;*Alb-Cre* mice fed regular chow at the age of 30 weeks (G). Representative images of livers (H), H&E staining (I), and serum ALT, ALP and TBil levels (J) from *Prkcz*$^{f/f}$ and *Prkcz*$^{f/f}$;*Alb-Cre* mice (n = 3-6). (K-P) *Prkcz*$^{f/f}$;*Alb-Cre* mice subjected to DEN/HFD protocol. Schematic representation of DEN/HFD-induced HCC model. Two-week-old *Prkcz*$^{f/f}$ and *Prkcz*$^{f/f}$;*Alb-Cre* mice were intraperitoneally injected with diethylnitrosamine (DEN, 25 mg/kg) and two weeks later were fed 60% fat diet for 32 weeks (K). Representative images of livers from *Prkcz*$^{f/f}$ and *Prkcz*$^{f/f}$;*Alb-Cre* mice (L). H&E staining of *Prkcz*$^{f/f}$ and *Prkcz*$^{f/f}$;*Alb-Cre* livers (M). Total number of tumors (N) and maximal tumor diameters (O) in *Prkcz*$^{f/f}$ and *Prkcz*$^{f/f}$;*Alb-Cre* livers (n = 8-13). Frequencies of liver adenoma, HCC and lung metastasis in *Prkcz*$^{f/f}$ and *Prkcz*$^{f/f}$;*Alb-Cre* male mice (P). (Q) ^{13}C contribution to lipogenic acetyl-CoA pool from [U-$^{13}C_6$]glucose over 24 h in sg*Prkci* (#1 and #2) and sgC BNL CL.2 cells (n = 3). (R) Isotopologue distribution of intracellular palmitate (M0 to M16 according to labeled carbons) from [U-$^{13}C_6$]glucose over 24h in sg*Prkci* (#1 and #2) and sgC BNL CL.2 cells (n = 3). Results are presented as mean ± SEM with exception of (J), in which data is presented as mean ± 95% confidence interval. *$p < 0.05$, **$p < 0.01$, ***$p < 0.001$. Scale bar, 1cm (H and L); 100 μm (I and M).

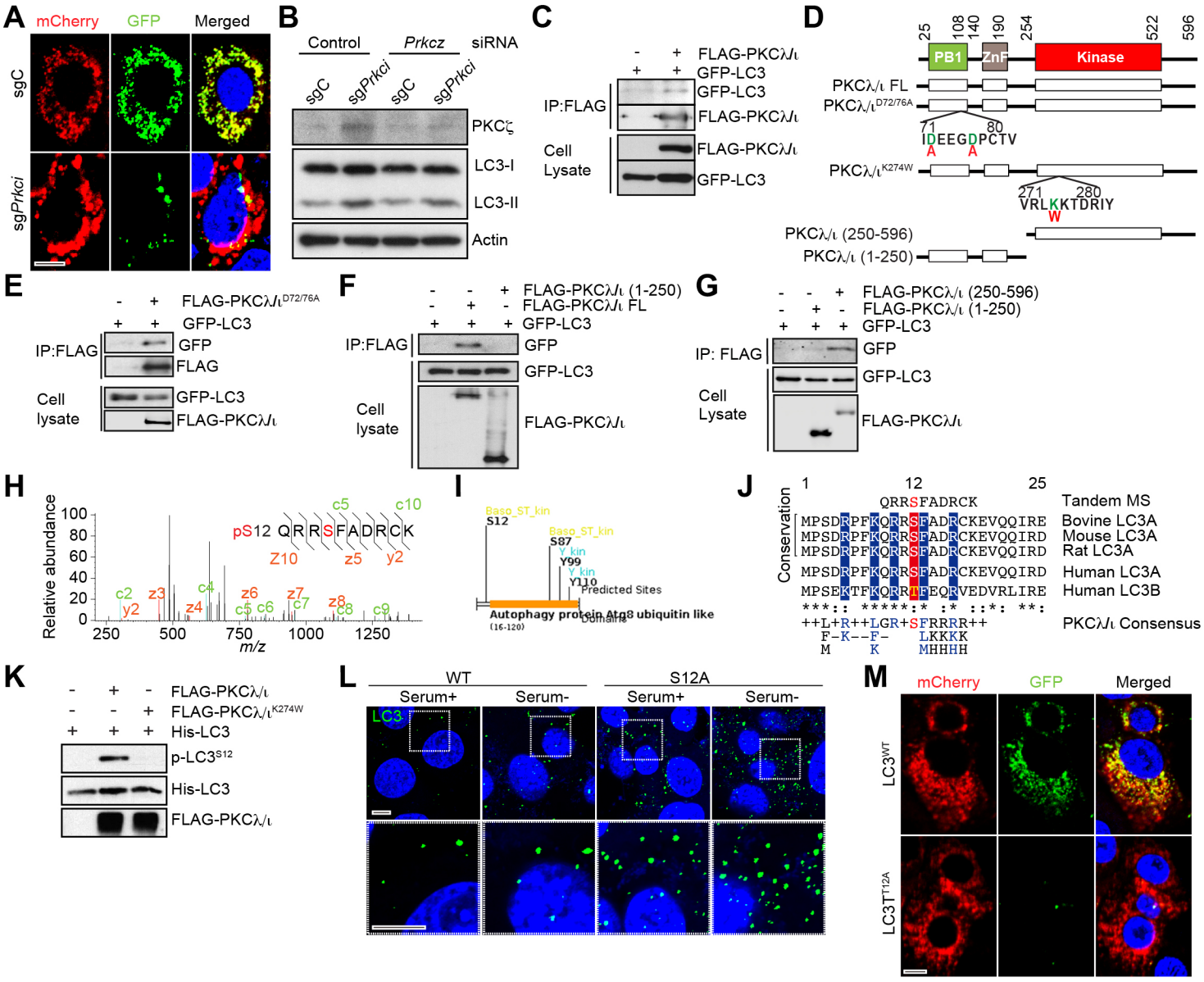

Figure S5. PKCλ/ι Phosphorylates LC3 to Suppress Autophagy, Related to Figure 4

(A) Representative IF images of sg*Prkci* and sgC BNL CL.2 cells in response to 4 hours of FBS starvation using tandem mCherry-GFP-tagged LC3B reporter plasmid. (B) Immunoblotting for LC3 of cell lysate from sg*Prkci* and sgC BNL CL.2 cells with *Prkcz* siRNA or control siRNA transfection. (C) Immunoblotting of cell lysate and FLAG-tagged immunoprecipitates of HEK293T cells transfected with indicated constructs. (D) Schematic representation of domain structure of human PKCλ/ι and plasmid used in this study. (E) Immunoblotting of cell lysate and FLAG-tagged immunoprecipitates of HEK293T cells transfected with LC3 and wild-type PKCλ/ι or mutant PKCλ/ι$^{D72/76AA}$ that abolishes its binding to p62. (F) Immunoblotting of cell lysate and FLAG-tagged immunoprecipitates of HEK293T cells transfected with LC3 and PKCλ/ι lacking kinase domain (FLAG-PKCλ/ι (1-250)) or PKCλ/ι full length (FLAG-PKCλ/ι FL). (G)

Immunoblotting of cell lysate and FLAG-tagged immunoprecipitates of HEK293T cells transfected with LC3 and kinase domain of PKCλ/ι (FLAG-PKCλ/ι (250-596)) or kinase domain deficient PKCλ/ι (FLAG-PKCλ/ι (1-250)). (H) MS/MS spectra of human LC3 peptide phosphorylated by human PKCλ/ι. (I) Predicted phosphorylation sites in human LC3 by ScanSite v4.0 software. (J) Alignment of the amino acid sequence of human LC3 (1-25 aa) with orthologs in other species, in comparison with PKCλ/ι consensus sequence. (K) *In vitro* kinase assay of LC3 with wild-type PKCλ/ι or kinase-dead mutant PKCλ/ι (PKCλ/ι^{K274W}). Phosphorylated Ser 12 in LC3 (p-LC3^{S12}) detection by immunoblotting. (L) IF for FLAG-tagged LC3 wild-type (WT) or S12A mutant (S12A) stably expressing BNL CL.2 cells cultured with or without serum for 4 h. (M) Representative IF images of BNL CL.2 cells in response to 4 h of FBS starvation using tandem mCherry-GFP-tagged LC3B wild-type (WT) or T12A mutant (T12A) reporter plasmid. Scale bar, 10 μm

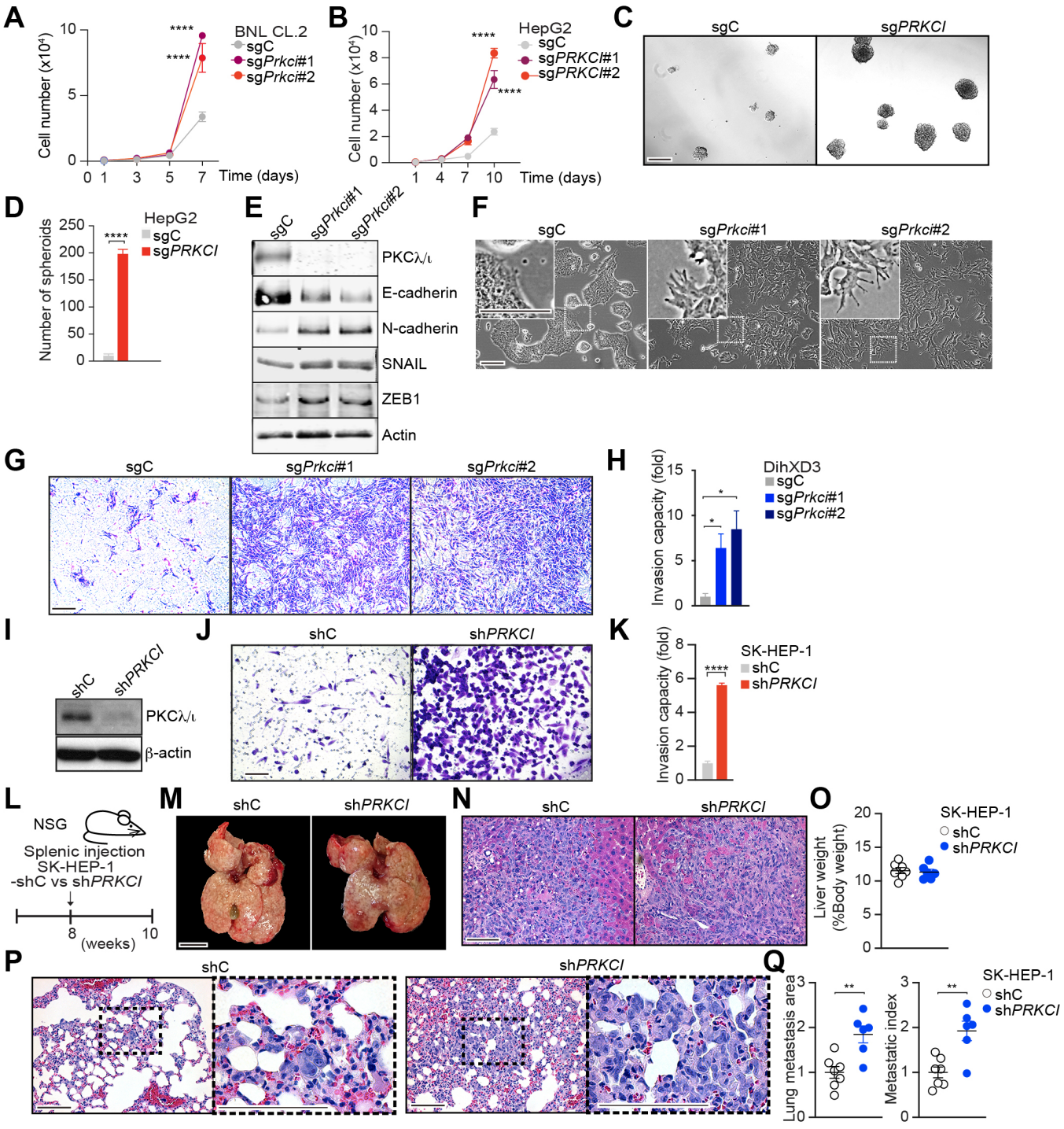

Figure S6. Loss of PKCλ/ι in Hepatoma Cells Promotes Cancer Invasiveness, Related to Figure 5

(A and B) Cell number of sg*Prkci* or sgC BNL CL.2 cells (A) and sg*PRKCI* or sgC HepG2 cells (B) cultured in complete media (n = 3). (C and D) Sphere formation assay of sg*PRKCI* or sgC HepG2 cells. Representative images (C) and quantification of spheres (n = 4) (D). (E and F) EMT phenotypes of sg*Prkci* or sgC DihXD3 cells. Immunoblotting for EMT marker proteins (E) and cell morphology (F) in sg*Prkci* or sgC DihXD3 cells. (G and H) *In vitro* invasion assay of sg*Prkci* or

sgC DihXD3 cells. Representative images (G) and quantification of invasive cells (n = 3) (H). (I) Immunoblotting of PKCλ/ι protein in *PRKCI* gene knockdown (sh*PRKCI*) or control (shC) SK-HEP-1 cells, normalized to actin. (J and K) *In vitro* invasion assay of sh*PRKCI* or shC SK-HEP-1 cells. Representative images (J) and quantification of invasive cells (n = 3) (K). (L-Q) Schematic representation of sh*PRKCI* or shC SK-HEP-1 cells transplantation through splenic injection in NSG mice (L). Representative images of livers (M) and H&E staining of livers (N) injected with sh*PRKCI* or shC SK-HEP-1 cells. Quantification of liver weight normalized to body weight (shC, n = 7; sh*PRKCI*, n = 6) (O). Representative H&E images of lungs (P) and quantification of lung metastasis area per filed. The metastatic index was defined as the ratio of the metastasis area over the size of the primary lesions represented by normalized liver size (Q). Results are presented as mean ± SEM. *$p < 0.05$, **$p < 0.01$, ***$p < 0.001$. Scale bar, 100 μm (C, F, G, J, N, and P); 1 cm (M).

Table S1. Primer sets for qRT-PCR analyses, Related to STAR METHODS

Gene Symbol	Forward	Reverse
18s rRNA	GTAACCCGTTGAACCCATT	CCATCCAATCGGTAGTAGCG
Acadl	GGGAATGAAAGCTCAGGACA	AGAATCCGCATTAGCTGCAT
Acadm	AGGTTTCAAGATCGCAATGG	CATTGTCCAAAAGCCAAACC
Acads	TGGCGACGGTTACACACTG	GTAGGCCAGGTAATCCAAGCC
Acot1/2	GACAAGAAGAGCTTCATTCCCGTG	CATCAGCATAGAACTCGCTCTTCC
Cpt1a	CGGTGGAACAGGATCCGAG	TCACGTGACGGCTGAGAAAA
Crat	TCAAAGGCATGGGTGACTCC	TCGGATGGCCCGGTCAG
Ehhadh	GGACCATACGGTTAGAGCCA	ATGGATATCAGCACCTGCACA
Glrx	CTGCAGTTATAAAAGGGGTGGC	ACTGACATCCTCTGCGATGC
Gpx2	ACTACCCGGGACTACAACCA	TGACAGTTCTCCTGATGTCCG
Gsr	TGGCACTTGCGTGAATGTTG	AGCCGTAATCCACGTGATCG
Gsta1	CTGGACTGTGAGCTGAGTGG	CATTGAAGTAGTGAAGCACG
Gsta2	TGAAAAGGTGTTGAAGAGCCA	AGAAGGCTGGCATCAAGCTC
Hmgcs2	AGAGGCCTTCAGGGGTCTAA	TTGAACATGTCCAGGGAGGC
Nqo1	AGCGTTCGGTATTACGATCC	AGTACAATCAGGGCTCTTCTCG
Ppara	GACGCTTGTGGCCAAGAT	GTGATAAAGCCATTGCCGT
Ppargc1a	GGCTAGTCCTTCCTCCATGC	TTGGCTGGTGCCAGTAAGAG
Ppargc1b	TCAACTATCTCGCTGACACGC	GAGTTCTCTGGGCACCACTG
Prkcz	TACACTCCTGCTTCCAGACA	CTCAGCAGCATAGAACCTGG
Txnrd1	CAGCCCTGAAGCCGAACAAA	GTCATAGGACCCAGGGGGAT